

MODELING SEASONALITY AND SERIAL DEPENDENCE OF ELECTRICITY PRICE CURVES WITH WARPING FUNCTIONAL AUTOREGRESSIVE DYNAMICS¹

BY YING CHEN^{*}, J. S. MARRON^{*,†,2} AND JIEJIE ZHANG^{*}

National University of Singapore^{} and University of North Carolina[†]*

Electricity prices are high dimensional, serially dependent and have seasonal variations. We propose a Warping Functional AutoRegressive (WFAR) model that simultaneously accounts for the cross time-dependence and seasonal variations of the large dimensional data. In particular, electricity price curves are obtained by smoothing over the 24 discrete hourly prices on each day. In the functional domain, seasonal phase variations are separated from level amplitude changes in a warping process with the Fisher–Rao distance metric, and the aligned (season-adjusted) electricity price curves are modeled in the functional autoregression framework. In a real application, the WFAR model provides superior out-of-sample forecast accuracy in both a normal functioning market, Nord Pool, and an extreme situation, the California market. The forecast performance as well as the relative accuracy improvement are stable for different markets and different time periods.

1. Introduction. Starting in the early 1980s, electricity markets have initiated reforms including liberalisation, privatisation, and restructuring of the energy supply and distribution industry that was traditionally monopolistic and government-controlled. As electricity is nonstorable, power system stability requires a constant balance between production and consumption. An over- or under-contracting and the need to rebalance are accompanied with large losses. This makes the forecast of electricity prices, especially within the next 24 to 48 hours, relevant to industry and academics alike.

Electricity prices are quoted at high frequency, that is, 24 hours a day, and 7 days a week, and exhibit a strong degree of serial dependence driven by, for example, common working time, demand and supply balance, economic and industrial developments. Moreover, electricity prices have unique seasonal features not observed in many other markets. The nature of business intensity and economic routine cause diurnal patterns, for example, with peak prices at middays and valleys in late evenings in the Nord Pool market as well as the California market, while the shifts of waking time from weekdays to weekends further introduce the shape variations in the electricity price curves.

Received February 2018; revised November 2018.

¹Supported by Singapore Ministry of Education Academic Research Fund Tier 1 and Institute of Data Science at National University of Singapore.

²Supported by the Saw Swee Hock Visiting Professorship.

Key words and phrases. Seasonal functional time series, warping function, Karcher mean.

There is a rich literature on Electricity Price Forecasting (EPF) models; see, for example, Skantze and Ilic (2012), Weron (2014). Fundamental models are in line with the standard demand and supply equilibrium. They are capable of incorporating linear or nonlinear supply stack and exogenous physical and economic factors such as loads, fuel prices, wind power and temperature to describe the price dynamics; see Vehviläinen and Pyykkönen (2005), Kanamura and Ōhashi (2007), Boogert and Dupont (2008), Kanamura and Ōhashi (2008), Howison and Coulon (2009), Amjady and Keynia (2009), Amjady, Daraeepour and Keynia (2010), Nowotarski and Weron (2015), Gaillard, Goude and Nedellec (2016), Maciejowska and Nowotarski (2016), Juban et al. (2016), Maciejowska, Nowotarski and Weron (2016), Pape, Hagemann and Weber (2016) and Bello et al. (2016).

Autoregressive models account for the serial dependence among the historical, present and future values of electricity prices and have been widely used with success in electricity price forecast. Compared to the fundamental models with finite explanatory variables, the time series models indirectly consider the impact of all the potential driving factors, by incorporating the historical values as predictors that are most likely influenced by the same factors in a similar way; see also the AutoRegressive Moving Average with eXogenous variable (ARMAX) (Nogales et al. (2002)), the AutoRegressive Integrate Moving Average (ARIMA) and the ARIMA-E (ARIMA with load as an explanatory variable) (Contreras et al. (2003)). The univariate models consider the 24 serially dependent hourly price processes separately, while the multiple series exhibit cross-dependence where the hourly price process depends on the historical values of another process. This seems to motivate the adoption of the multivariate time series analytical tools such as the Vector Autoregressive (VAR) models; see, for example, Lütkepohl (2005). The VAR models however yield unsatisfactory results, with moderate and often insignificant modeling parameters. This is to some extent caused by the overfitting that occurs when the model has excessively many parameters. In this case, the fitted model describes random noise instead of the underlying relationship. Multivariate factor models provide possible efficient solutions by representing the large dimensional data with a relatively small set of factors at a cost of little information loss; see, for example, Garcia-Martos, Rodriguez and Sánchez (2012), Liebl (2013) and Maciejowska and Weron (2016), and also the Vector Autoregressive-Threshold Autoregressive Conditional Heteroskedasticity (VAR-TARCH) approach with exogenous variables (Ziel, Steinert and Husmann (2015)).

Recent development on functional time series analysis provides an alternative way for analysing large dimensional electricity price processes by taking into account all the raw information. In the functional domain, a continuous daily price curve can be formed by smoothing over the 24 discrete hourly prices on each day. The serial cross-dependence among the daily price curves is modeled by the functional autoregressive (FAR) model, which extends the time series analysis from a finite dimensional space to an infinite world; see, for example, Bosq (2000). Bosq

(1991) derives a functional Yule–Walker (YW) estimator for the serially dependent functional data. Besse, Cardot and Stephenson (2000) propose a nonparametric kernel estimator based on a functional form of the YW equations; see also Antoniadis and Sapatinas (2003), Kokoszka and Zhang (2010) and Didericksen, Kokoszka and Zhang (2012). Mourid and Bensmain (2006) propose a maximum likelihood estimator of the FAR model using a sieve approximation. Chen and Li (2017) employ an adaptive approach to extend the maximum likelihood estimation to nonstationary situation and implement forecast experiments on California electricity prices. The adaptive FAR delivers superior forecast accuracy compared with several alternative models, including the univariate time series models of AR and ARX with load forecast and seasonal dummies as exogenous variables and the multivariate VAR model.

Despite good forecast accuracy, the (adaptive) FAR models essentially ignore the shifts of diurnal pattern from weekdays to weekends and unrealistically assume no seasonal variations from day to day. On the other hand, seasonality of electricity prices has been well studied in univariate time series models. Shahidehpour, Yamin and Li (2002) use historical data for days with characteristics, for example, the day of the week, the day of the year, holiday type, and weather/consumption figures that are similar to the predicted day to forecast future prices; see also Nogales et al. (2002) and Weron (2007). Hernandez et al. (2006) point out that the pattern of prices varies across day types. Koopman, Ooms and Carnero (2007) consider periodic seasonal regression models with fractional ARIMA and GARCH disturbances to address the yearly seasonal effect and the day-of-week effects for the analysis of daily electricity spot prices. Janczura et al. (2013) adopt a deseasonalization approach that treats the prices as a sum of a trend-seasonal component and a stochastic component. The econometric model introduced by Ziel, Steinert and Husmann (2015) assumes that some days have equal hourly mean components and consider five groups of parameter restrictions to address the weekly seasonal effects.

The seasonal variations entangle with the dynamic evolution of electricity price curves driven by, for example, demand and supply changes. In other words, there are eventually two dynamic movements in the series of electricity price curves. One is the amplitude evolution process driven by economic cycles and market restructuring, the other is the phase swings along the time axis within a day driven by the seasonal variations from weekdays to weekends. A separation of the amplitude and phase variations is of great interest in order to discover a broad common diurnal pattern of the daily price curves without the impact of day types; in addition, it helps to understand the seasonal impact on the price development and thus to enhance the forecast accuracy of electricity prices.

Time warping is a useful tool to separate amplitude and phase variations in functional domain, which is also known as functional alignment or curve registration. We refer to Marron et al. (2014) for a comprehensive review. Sakoe and Chiba

(1978) aligns two signals with different time-axis fluctuation in speech recognition, where the Euclidean distance metric is employed as a measure of the difference between two signals. Kneip and Gasser (1992) introduces a landmark method, which warps the special features such as peak locations to their average location and then smooth transformations from the average location to the location of the feature; see also Gasser and Kneip (1995). Wang, Chiou and Müller (2016) points out that sometimes the landmarks may be missing or hard to identify. Wang and Gasser (1997) advances the accuracy of dynamic time warping by incorporating a cost function.

A proper choice of distance metric and template function is of high importance in time warping. Many earlier approaches to this problem use standard distance on curve space such as \mathcal{L}^2 . This can lead to unsatisfactory results, as shown in Figure 8 of Marron et al. (2015). Ramsay and Li (1998) also points out that the cross-sectional mean curve is not a good representative of the sample of curves with phase variation. A much more stable approach, with solid mathematical underpinning, is a metric which is warp invariant, such as the Fisher–Rao metric as proposed in Srivastava et al. (2011); see also Radhakrishna Rao (1945), Efron (1975), Čencov (1982), Kass and Vos (2011). As noted in Srivastava et al. (2011) and Marron et al. (2014), the Fisher–Rao method is especially good at aligning peaks and valleys.

We propose a Warping Functional AutoRegressive (WFAR) model for the dynamic electricity price curves with seasonality. In a warping procedure, the (seasonal) phase variation and the amplitude change of electricity price curves are separated using the Fisher–Rao metric. The dynamics of the aligned curves, after removing seasonal variations, are described by the functional autoregressive model. The forecasts of price curves are obtained by warping back the deseasonalized curve forecasts with the respective warping functions of the same day type. The WFAR model simultaneously accounts for cross time-dependence and seasonal variations of the large dimensional data measured at high time resolution, namely every hour. It is general and can be used for modeling and forecasting other functional time series with seasonality. In a real application, the WFAR model provides superior out-of-sample forecast accuracy in both a normal functioning market, Nord Pool, and an extreme situation, the California market. The forecast performance as well as the relative accuracy improvement are stable for different markets and different time periods.

This paper is structured as follows. Section 2 describes the electricity price data in the Nord Pool market and the California market. Section 3 details the WFAR model including the Fisher–Rao metric, warping process and FAR estimation. Section 4 exercises the real data analysis for both in-sample and out-of-sample evaluation. Section 5 concludes.

2. Data. We consider two data sets: the hourly electricity prices in the Nord Pool market from 1 January 2013 to 31 December 2017 and the California market

from 5 July 1999 to 31 January 2001. The Nord Pool data contain a long period and are used to demonstrate the performance of the proposed WFAR model in a normal functioning market situation. The data are downloaded from the Nord Pool official site, <http://www.nordpoolspot.com/historical-market-data/>. In our study, the hourly price is actually system price that is an unconstrained market clearing reference price calculated without any congestion restrictions by setting capacities to infinity. The system price is considered by most standard contracts traded in the Nordic region as reference price (<https://www.nordpoolgroup.com>). The California market data illustrate the performance of the WFAR model in an extreme situation as there was a famous California electricity crisis that led to an explosion in electricity prices from May 2000 to June 2001 (Joskow (2001)). The California market data can be downloaded from <http://www.caiso.com>. To avoid the impact of extreme spikes and deal with 0 prices, we take the shifted base 10 logarithmic transformation of the raw data. Suggested by the referee, we consider use of $\log_{10}(\text{price} + a)$ with $\text{price} + a > 1$ for the log transformation of a close-to-zero price will lead to a very large negative value and thus “spurious” negative spike; see Feng, Hannig and Marron (2016) for further discussion. For other possible transformations, we refer to Uniejewski, Weron and Ziel (2018) for more details.

Figure 1(a) shows the 3D surface plot of the hourly log electricity prices of the Nord Pool market from 1 January 2013 to 31 December 2017, which is generally flat over the 5-year period. In contrast, the 3D surface plot of the hourly log prices of the California market from 5 July 1999 to 31 January 2001 in Figure 1(b) was more volatile over the 2-year period. As can be seen in Figure 1(b), the \log_{10} prices were under 2.35 before 5 April 2000 (close to but before the California electricity crisis), and boomed up to 3.4 (a 10 fold increase) during the California electricity crisis (from May 2000 to June 2001). The daily log price curves are obtained

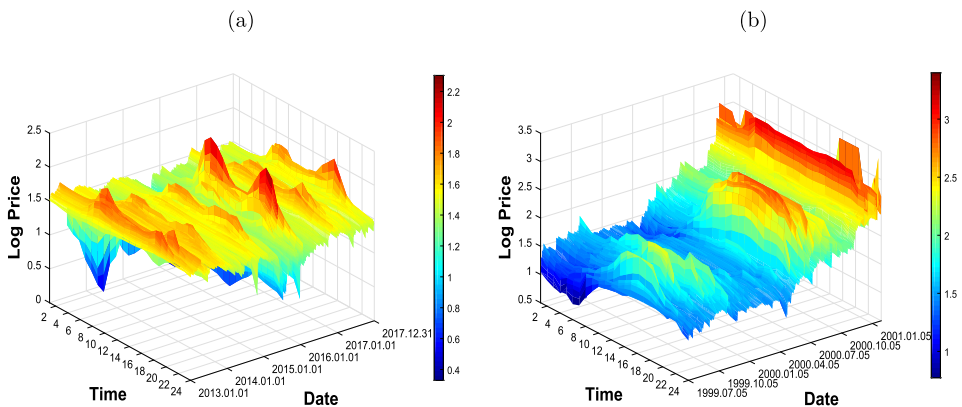


FIG. 1. Overview: (a) 3D surface plot of the hourly log electricity prices of the Nord Pool market from 1 January 2013 to 31 December 2017; (b) 3D surface plot of the California market from 5 July 1999 to 31 January 2001.

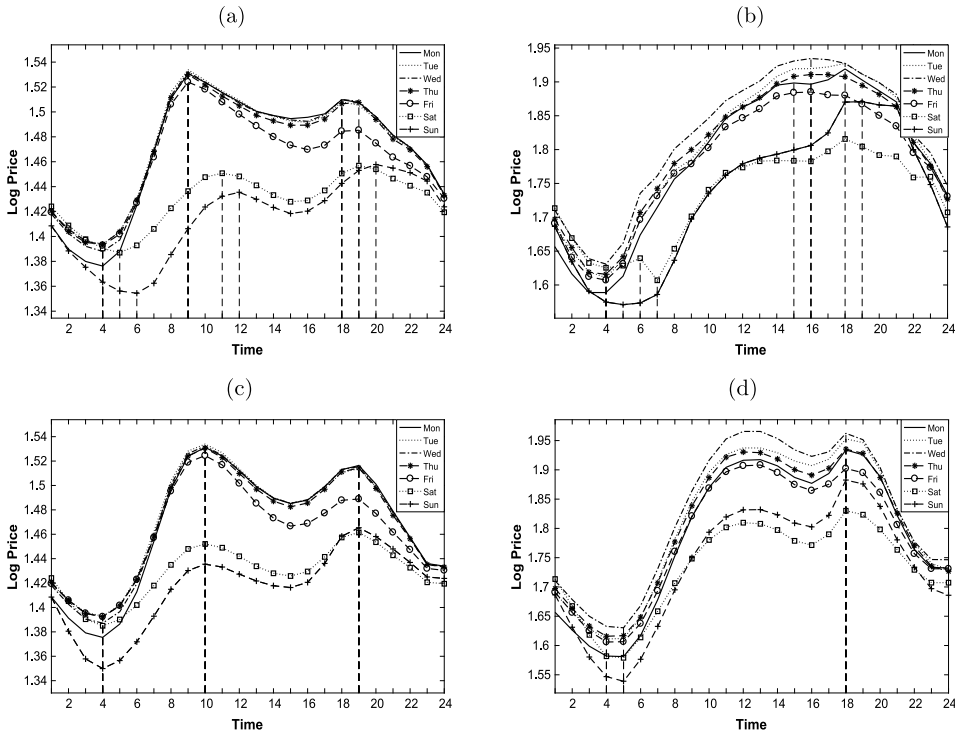


FIG. 2. Average of unwarped (a) and warped (c) hourly log prices on different days of the week in the Nord Pool market from 1 January 2013 to 31 December 2017; Average of unwarped (b) and warped (d) hourly log prices on different days of the week in the California market from 5 July 1999 to 31 January 2001. There are differences on both curve levels and curve phase features like peaks and valleys between weekdays and weekends.

by smoothing over 24 discrete points via the Fourier expansion with 23 basis elements. The diurnal pattern can be easily visualized in Figure 2(a) and 2(b), where the average values of the unwarped hourly prices on different days of the week for the Nord Pool market and the California market are computed, respectively. In Figure 2(a), the peaks occur during 18:00–20:00 and 9:00–12:00, and the valleys are between 4:00 and 6:00 in the Nord Pool market. The peaks of the California market occur during 15:00–19:00 with the valleys between 4:00 and 7:00. Beyond the diurnal pattern existing in the price curves, there is simultaneously a shift of diurnal pattern between weekdays and weekends. Such seasonal phase variations are illustrated by the comparison between the average values of the unwarped and warped hourly prices on different days of the week in each market; see the Nord Pool market in Figure 2(a) and 2(c), and the California market in Figure 2(b) and 2(d), respectively. In the cases of unwarped curves, the existence of seasonal variations obscures the shape of diurnal pattern, when taking averages over different day types, and the peaks/valleys occur later on weekends than weekdays. After

time warping, which adjusts the seasonality but leaves the amplitude distance of price curves unchanged, the peaks and valleys are aligned as shown in Figure 2(c) and Figure 2(d), respectively.

Some summary statistics of the 24 hourly log price series are shown in Figure 3, with the Nord Pool market over the 5-year period in the left panel and the California market over the 2-year period in the right panel. The minimum prices of both markets happen around 2:00 to 6:00 and there are no negative prices in either sample period; see Figure 3(a) and Figure 3(b). The maximum hourly prices of the Nord Pool market has two peaks around 9:00 and 18:00 shown in Figure 3(c). In the California market, the maximum hourly prices appeared at 18:00–21:00; see Figure 3(d). The spike at midnight happened on 22 January 2001 with a raw price of 2499.0 during the California electricity crisis. The hourly prices are on average high around 16:00–21:00 and low at midnight from 1:00 to 5:00 in both markets; see Figure 3(e) and 3(f). The standard deviations of both markets, on the other hand, are stable.

There exists a strong degree of serial dependence in electricity prices. As an illustration, Figure 4(a) and Figure 4(b) depict the time series plots of two hourly price series at 17:00 and 18:00 of the Nord Pool market and the California market, respectively, which show obvious comovement. Compared to the concurrent dependence, the lead-lag dependence between the two series is practically more relevant in the forecast experiment. Figures 4(c) to 4(f) show clear evidence of positive autocorrelations and cross-correlations of the price series. Both measurements are significant even for large time lags, indicating that the electricity price at a particular hour not only depends on its own past values, but also the lagged values of other price series at a different hour. The sample measurements further demonstrate the existence of (weekly) seasonal variation, where a hump is repeated at every 7 lags, implying even stronger serial dependence among the same day of the week. The respective humps are strongest in the Nord Pool market; see Figure 4(c) and 4(e).

3. Method. In this section, we present the Warping Functional AutoRegressive (WFAR) model to simultaneously account for phase and amplitude variations of functional time series with seasonality. The phase variation driven by seasonality is separated in a warping process, where the Fisher–Rao Riemannian metric is used in order to preserve amplitude distance between curves. The serial dependence of the warped curves, after removing the impact of seasonality, can be safely modeled by functional autoregressive dynamics.

Let $\{X_t(\tau)\}_{t=1}^n$ denote a sequence of random curves over a time domain $\tau \in [0, 1]$ without loss of generality. The curves are continuous functions taking values in the Hilbert space \mathcal{H} endowed with its Borel σ -algebra $B_{\mathcal{H}}$. In our study, $X_t(\tau)$ is the daily price curve observed on day t , $t = 1, \dots, n$. We incorporate the empirical features of the electricity prices, namely seasonality w.r.t. day of the week, and propose an approach in estimating the warping functions. We classify the warping

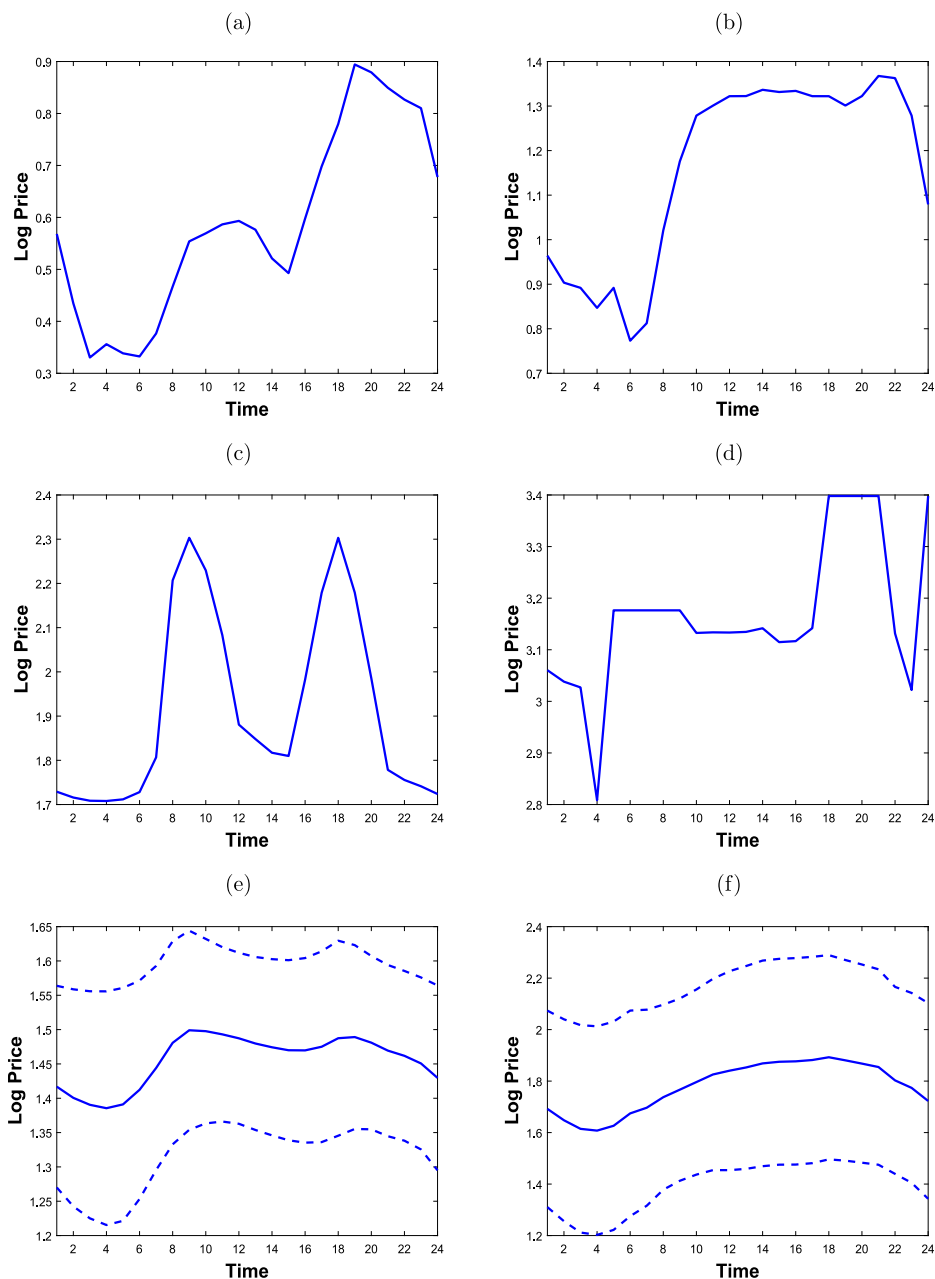


FIG. 3. Descriptive statistics of the Nord Pool market from 1 January 2013 to 31 December 2017 (left) and the California market from 5 July 1999 to 31 January 2001 (right). (a) and (c): Minimum and maximum of hourly log electricity prices of the Nord Pool market, respectively; (b) and (d): Minimum and maximum of hourly log electricity prices of the California market, respectively; (e): Mean \pm standard deviation of the hourly log electricity prices of the Nord Pool market; (f): Mean \pm standard deviation of the hourly log electricity prices of the California market.

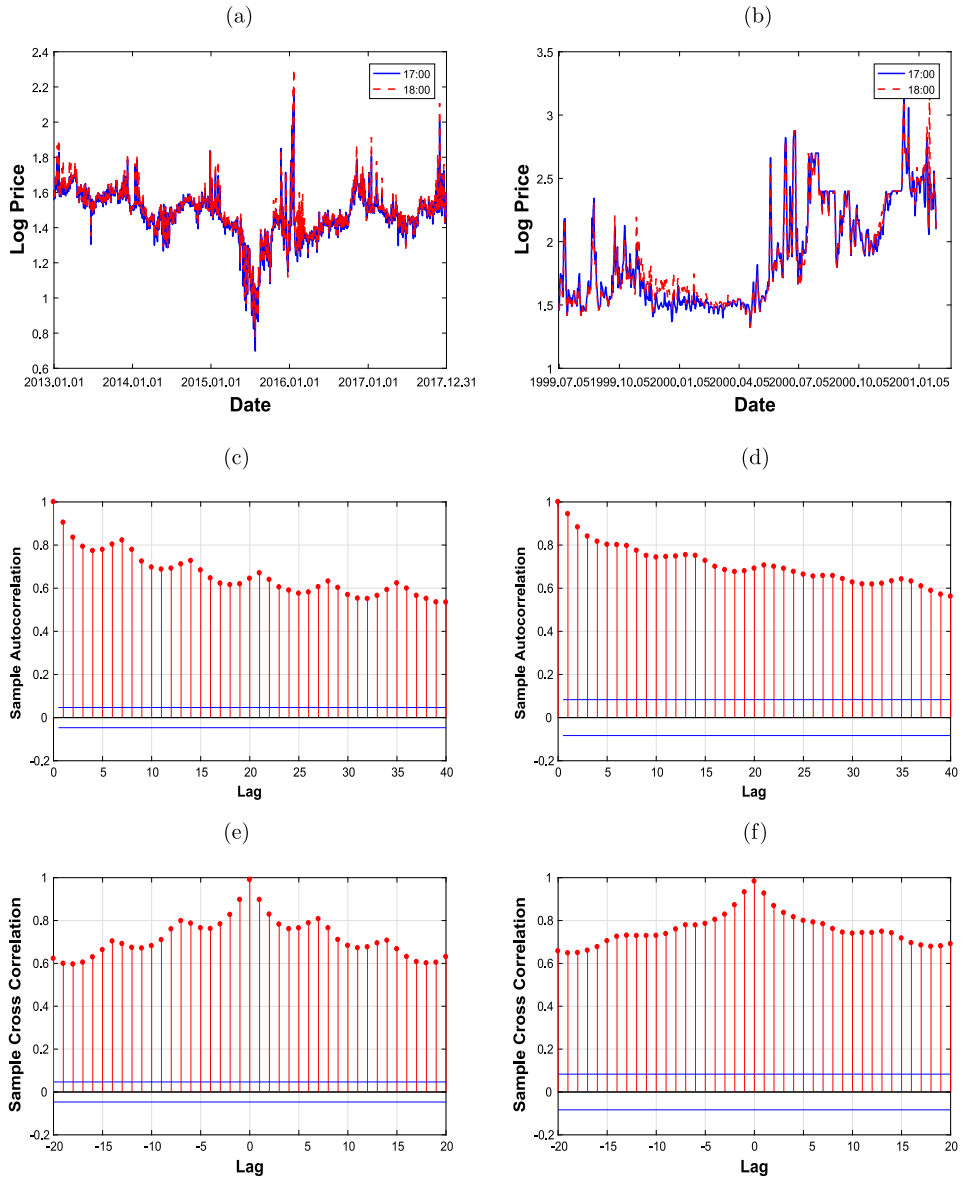


FIG. 4. *Serial dependence of the Nord Pool market from 1 January 2013 to 31 December 2017 (left) and the California market from 5 July 1999 to 31 January 2001 (right). (a) and (b): Time series plots of the hourly log prices at 17:00 and 18:00 o'clock of the Nord Pool market and the California market, respectively. In both markets, there is a strong cross correlation between the two adjacent hourly price series. (c) and (d): The sample auto-correlation functions of the hourly log prices at 17:00 of the Nord Pool market and the California market, respectively. The high ACF values indicate the dependence on the past prices at the same hour. (e) and (f): The sample cross correlation functions between the two hourly log price series at 17:00 and 18:00 of the Nord Pool market and the California market, respectively, which show evidence of the lead-lag serial dependence.*

functions into seven groups accordingly. We denote the (seasonal) warping functions as $\gamma^{(s)}$, where day type s refers to Monday to Sunday and $X_t^{(s)}(\tau)$ as the daily price curve on day t that belongs to day type s . The WFAR model is defined as follows:

$$(1) \quad Y_t^{(s)}(\tau) = X_t^{(s)} \circ \gamma^{(s)}(\tau),$$

$$(2) \quad Y_t(\tau) - \mu_Y(\tau) = \rho(Y_{t-1}(\tau) - \mu_Y(\tau)) + \varepsilon_t(\tau),$$

where $Y_t^{(s)}(\tau)$ denotes the warped (aligned) curve of $X_t^{(s)}(\tau)$ obtained in the warping process $X_t^{(s)} \circ \gamma^{(s)}(\tau)$, which registers the curve values at equal distant grids defined by the warping function $\gamma^{(s)}$. The serial dependence of the warped curves is modeled with the FAR model, where $\mu_Y(\tau)$ denotes the mean function of the warped curves, ρ is a Hilbert–Schmidt operator describing the serial dependence and $\varepsilon_t(\tau)$ is a strong \mathcal{H} -white noise with zero mean and finite second moment $E\|\varepsilon_t(\tau)\|^2 < \infty$.

In the following, we will present how to separate the seasonal phase variations in the warping process (1) and estimate the FAR operator using the maximum likelihood method in (2) under sieve—a reduced parameter space. The fitted model is then used in the forecast experiment.

3.1. *Warping and Fisher–Rao Riemannian metric.* The goal here is to separate phase and amplitude components of functional data in a proper way so that the amplitude remains unchanged in the warping process. We follow the nonparametric approach proposed by [Srivastava et al. \(2011\)](#). Let Γ be the set of warping functions: $\Gamma = \{\gamma : [0, 1] \rightarrow [0, 1] | \gamma(0) = 0, \gamma(1) = 1, \gamma \text{ is a diffeomorphism}\}$. The metric used in the warping process should satisfy the isometry property, that is, the distance between two functions remains the same given a common warping function:

$$(3) \quad \|X_i(\tau) - X_j(\tau)\| = \|(X_i \circ \gamma(\tau)) - (X_j \circ \gamma(\tau))\|,$$

for any $i, j \in \{1, \dots, n\}$ and $\gamma \in \Gamma$. The notation $\|\cdot\|$ denotes distance metric. The Fisher–Rao Riemannian metric ([Radhakrishna Rao \(1945\)](#)) is such a metric that preserves amplitude distance to warping; see [Čencov \(1982\)](#).

Let \mathcal{F} be the set of all absolutely continuous functions on $[0, 1]$. For any $X(\tau) \in \mathcal{F}$ and $v_1, v_2 \in T_X(\mathcal{F})$, where $T_X(\mathcal{F})$ is the tangent space to \mathcal{F} at $X(\tau)$, the Fisher–Rao Riemannian metric is defined as

$$(4) \quad d_{FR}(v_1, v_2) = \frac{1}{4} \int_0^1 v_1(\tau) v_2(\tau) \frac{1}{\dot{X}(\tau)} d\tau,$$

where $\dot{X}(\tau) = \frac{d}{d\tau} X(\tau)$. We drop the time point t here for notational simplification. Defined as a smoothly varying inner product on tangent spaces of a manifold, it is complicated to compute the F–R distance.

A square-root slope function (SRSF) representation has been proposed to simplify the computation; see [Kass and Vos \(2011\)](#) and [Čencov \(1982\)](#) for strictly positive functions and [Srivastava et al. \(2011\)](#) for extension to general functions. For any function $X(\tau) \in \mathcal{F}$, its SRSF takes the form:

$$(5) \quad q(\tau) = \dot{X}(\tau) / \sqrt{|\dot{X}(\tau)|}$$

which is invertible. Given the initial value $X(0)$ and the SRSF $q(\tau)$, one obtains $X(\tau) = X(0) + \int_0^\tau q(s)|q(s)| ds$. For the warped function $X \circ \gamma$, its SRSF takes the form

$$(6) \quad \tilde{q}(\tau) = (q \circ \gamma)(\tau)\sqrt{\dot{\gamma}(\tau)} = (q, \gamma).$$

[Srivastava et al. \(2011\)](#) shows that under the SRSF representation the F–R distance can be equivalently computed as conventional \mathcal{L}^2 metric. In other words, the F–R distance can be computed using the SRSFs of the original functions:

$$(7) \quad d_{FR}(X_i(\tau), X_j(\tau)) = \|q_i(\tau) - q_j(\tau)\|,$$

where the isometry property still holds:

$$(8) \quad \|q_i(\tau) - q_j(\tau)\| = \|(q_i, \gamma) - (q_j, \gamma)\| = \|\tilde{q}_i(\tau) - \tilde{q}_j(\tau)\|.$$

Given a set of functions X_1, X_2, \dots, X_n and letting q_1, q_2, \dots, q_n denote their SRSFs, the warping functions γ are chosen to minimize the distance of the phase-removed warped functions. Suppose a template function μ_X^* is known, which does not need to be warped or in other words its warping function is the identity $\gamma_{id}(\tau) = 1$. For any function X_t with $t = 1, \dots, n$, the warping function can be solved:

$$(9) \quad \gamma_t^* = \operatorname{argmin}_{\gamma \in \Gamma} d_{FR}(\mu_X^* - X_t \circ \gamma) = \operatorname{argmin}_{\gamma \in \Gamma} \|q_\mu^* - (q_t, \gamma)\|,$$

where q_μ^* is the SRSF of the template, which is computable in (5) when μ_X^* is provided.

In practice the template function is unknown, and the center of the functions is used as a template. Unlike many other scalar variables, the electricity price curves cannot necessarily be added given the existence of seasonality and hence the conventional mean is inappropriate. [Tang and Müller \(2008\)](#) defines the center to be a curve having the identity Karcher mean $\gamma_{id}(\tau) = 1$. The Karcher mean, also named Fréchet mean or Riemannian geometric mean ([Bhatia and Holbrook \(2006\)](#)) is a geometric mean of several matrices or functions that determines the “center” of a mass distribution on a Riemannian manifold. To obtain the center, a (temporal) template is computed by minimizing its overall F–R distances to all the functional data:

$$(10) \quad \mu_X = \operatorname{argmin} \sum_{t=1}^n \|\mu - (q_t \circ \gamma)\sqrt{\dot{\gamma}}\|.$$

Using μ_X as the (temporal) template function, one obtains the warping functions $\gamma_1, \gamma_2, \dots, \gamma_n$. This is equivalent to

$$(11) \quad \gamma_t = \underset{\gamma \in \Gamma}{\operatorname{argmin}} d_{\text{FR}}(\mu_X - X_t \circ \gamma) = \underset{\gamma \in \Gamma}{\operatorname{argmin}} \|q_\mu - (q_t, \gamma)\|,$$

where q_μ is the SRSF of μ_X . The warping function γ_t actually indicates how the X_t is warped and the linear interpolation of X_t at γ_t is used in implementing the warping process $X_t \circ \gamma$. When aligning to μ_X , however, the warping functions do not necessarily have the identity Karcher mean. To obtain the center μ_X^* whose corresponding warping functions $\gamma_1^*, \gamma_2^*, \dots, \gamma_n^*$ have the identity Karcher mean γ_{id} , one needs to update the warping functions by modifying the shooting vector that represents the direction of the warping. The algorithm is formulated as in Srivastava et al. (2011):

ALGORITHM (Srivastava et al. (2011)).

1. For every γ_t , compute its SRSF $\psi_t = \sqrt{\gamma_t}$;
2. Initialize $\mu_\psi = \psi_j$, where j is such that $\operatorname{argmin}_{1 \leq i \leq n} \|\psi_i - \frac{1}{n} \sum_{t=1}^n \psi_t\|$;
3. For each ψ_t , compute the shooting vectors $v_t = \frac{\theta_t}{\sin(\theta_t)}(\psi_t - \cos(\theta_t)\mu_\psi)$, where $\theta_t = \cos^{-1}(\int_0^1 \mu_\psi(\tau)\psi_t(\tau) d\tau)$;
4. Compute average direction $\bar{v} = \frac{1}{n} \sum_{t=1}^n v_t$;
5. If $\|\bar{v}\|$ is small, stop. Else, update $\mu_\psi \mapsto \cos(\epsilon \|\bar{v}\|)\mu_\psi + \sin(\|\bar{v}\|) \frac{\bar{v}}{\|\bar{v}\|}$ for a small step size $\epsilon > 0$ and return to 3;

Compute the Karcher mean $\bar{\gamma}_n = \int_0^\tau [\mu_\psi(z)]^2 dz$. The interpolated values of each γ_t at query points are specified by $\bar{\gamma}_n^{-1}$, which return the estimates $\gamma_1^*, \gamma_2^*, \dots, \gamma_n^*$. We assume the seasonal phase variation constant and use the fixed seasonal warping function $\gamma^{(s)}$ for day type s in the time warping process. In this way, all the time-dependent variations in the price curves are pushed into the amplitude variations. We categorize $\gamma_1^*, \gamma_2^*, \dots, \gamma_n^*$ into seven groups according to their day types and take the Karcher mean of each group as the final warping function, that is, the estimate of $\gamma^{(s)}$,

$$(12) \quad \gamma^{(s)} = \int_0^\tau [\mu_\psi^{(s)}(z)]^2 dz,$$

where day type s is from Monday to Sunday and $\mu_\psi^{(s)}(z)$ is obtained via Algorithm [Srivastava et al. (2011)] for the day type s . The warped (seasonal-adjusted) curves are obtained via $Y_t^{(s)} = X_t^{(s)} \circ \gamma^{(s)}$ in equation (1), where $\gamma^{(s)}$ is the warping function for day $t, t = 1, \dots, n$.

3.2. *FAR model and sieve estimator.* For the warped functions $Y_t(\tau)$ without phase variation, the Functional AutoRegressive (FAR) model can be safely employed to describe the time evolution. The FAR model is defined as in (2):

$$Y_t(\tau) - \mu_Y(\tau) = \rho(Y_{t-1}(\tau) - \mu_Y(\tau)) + \epsilon_t(\tau).$$

Represent the operator ρ using a convolution kernel operator K , where $K \in \mathbb{L}^2([0, 1])$ is an even function with $\|K\| < 1$, the FAR model has a form of

$$(13) \quad Y_t(\tau) - \mu_Y(\tau) = \int_0^1 K(\tau - s)[Y_{t-1}(s) - \mu_Y(s)] ds + \epsilon_t(\tau).$$

Expand each functional term in the FAR model with trigonometric basis functions:

$$\phi_0 = I_{[0,1]}, \quad \phi_{2k}(\tau) = \sqrt{2} \cos 2\pi k\tau, \quad \phi_{2k-1}(\tau) = \sqrt{2} \sin 2\pi k\tau.$$

We have

$$\begin{aligned} Y_t(\tau) &= a_{t,0} + \sum_{k=1}^{\infty} [b_{t,k} \phi_{2k-1}(\tau) + a_{t,k} \phi_{2k}(\tau)], \\ \epsilon_t(\tau) &= a_{t,0}(\epsilon_t) + \sum_{k=1}^{\infty} [b_{t,k}(\epsilon_t) \phi_{2k-1}(\tau) + a_{t,k}(\epsilon_t) \phi_{2k}(\tau)], \\ K(\tau) &= c_0 + \sum_{k=1}^{\infty} c_k \phi_{2k}(\tau), \\ \mu(\tau) - \int_0^1 K(\tau - s)\mu(s) ds &= p_0 + \sum_{k=1}^{\infty} [q_k \phi_{2k-1}(\tau) + p_k \phi_{2k}(\tau)], \end{aligned}$$

where $a_{t,0}$, $a_{t,k}$, $b_{t,k}$ are the Fourier coefficients associated with the warped functions, $a_0(\epsilon)$, $a_k(\epsilon)$, $b_k(\epsilon)$ are those for the unknown innovations, c_0 , c_k correspond to the unknown kernel function, and p_0 , p_k , q_k are related to the mean function.

Plugging into the FAR model, the relationship of the warped functions can be equivalently represented by these Fourier coefficients for $k = 1, 2, \dots, \infty$:

$$\begin{aligned} a_{t,0} &= p_0 + c_0 a_{t-1,0} + a_0(\epsilon_t), \\ a_{t,k} &= p_k + \frac{1}{\sqrt{2}} c_k a_{t-1,k} + a_k(\epsilon_t), \\ b_{t,k} &= q_k + \frac{1}{\sqrt{2}} c_k b_{t-1,k} + b_k(\epsilon_t). \end{aligned}$$

In other words, the FAR model can be estimated based on the above equations.

The likelihood function is however not well-defined in the infinite dimensional parameter space. Nevertheless, based on the Grenander (1981) theory of Sieves, Geman and Hwang (1982) propose a way to approximate the likelihood on the

parameters' subspaces or Sieves and establish general consistency. Mourid and Bensmain (2006) propose an approximation of the likelihood function under sieve, a subspace of the parameters. Chen and Li (2017) extend the ML estimation for a general case where the mean function and innovation variation can be also consistently estimated. We follow the above work and introduce a sieve to construct an approximation. Let Θ denote the original infinite parameter space and let $\{\Theta_{m_n}\}$, named sieves, be a sequence of subsets of Θ :

$$\Theta_{m_n} \subset \Theta_{m_{n+1}} \subset \dots \subset \Theta, \quad \text{and} \quad \bigcup \Theta_{m_n} \text{ is dense in the parameter space } \Theta.$$

Specifically,

$$\Theta_{m_n} = \left\{ K \in \mathbb{L}^2 \mid K(\tau) = c_0 I_{[0,1]}(\tau) + \sum_{k=1}^{m_n} c_k \sqrt{2} \cos 2\pi k\tau, \right. \\ \left. \tau \in [0, 1], \sum_{k=1}^{m_n} k^2 c_k^2 \leq m_n \right\},$$

where $1 \leq k \leq m_n, m_n \rightarrow +\infty$ as $n \rightarrow +\infty$.

Assume the Fourier coefficients of the innovation function $\epsilon_t(\tau)$, denoted as $a_0(\epsilon_t), a_k(\epsilon_t)$ and $b_k(\epsilon_t)$, are independent and identically Gaussian distributed with mean zero and variance σ_k^2 , we define a transition density

$$g(Y_t, Y_{t-1}, \rho) \\ = \frac{2\pi^{-(2m_n+1)/2}}{\sigma_0 \prod_{k=1}^{m_n} \sigma_k^2} \cdot \exp \left\{ -\frac{1}{2\sigma_0^2} (a_{t,0} - p_0 - c_0 a_{t-1,0})^2 \right. \\ \left. - \sum_{k=1}^{m_n} \frac{1}{2\sigma_k^2} \left[\left(b_{t,k} - q_k - \frac{1}{\sqrt{2}} c_k b_{t-1,k} \right)^2 \right. \right. \\ \left. \left. + \left(a_{t,k} - p_k - \frac{1}{\sqrt{2}} c_k a_{t-1,k} \right)^2 \right] \right\},$$

and thus the conditional log-likelihood $L(Y_1, \dots, Y_n; \rho)$ is

$$L(Y_1, \dots, Y_n; \rho) \\ = \log \left\{ \prod_{t=2}^n g(Y_t, Y_{t-1}, \rho) \right\} \\ = -\frac{(2m_n + 1)(n - 1)}{2} \log 2\pi - (n - 1) \log \sigma_0 - (n - 1) \sum_{k=1}^{m_n} \log \sigma_k^2 \\ - \frac{1}{2\sigma_0^2} \sum_{t=2}^n (a_{t,0} - p_0 - c_0 a_{t-1,0})^2$$

$$\begin{aligned}
 & - \sum_{t=2}^n \sum_{k=1}^{m_n} \frac{1}{2\sigma_k^2} \left\{ \left(b_{t,k} - q_k - \frac{1}{\sqrt{2}} c_k b_{t-1,k} \right)^2 \right. \\
 & \left. + \left(a_{t,k} - p_k - \frac{1}{\sqrt{2}} c_k a_{t-1,k} \right)^2 \right\}.
 \end{aligned}$$

By maximising the log-likelihood on the sieve $\{\Theta_{m_n}\}$ with a fixed m_n , we obtain the sieve estimator of the Fourier coefficients with a closed-form

$$\begin{aligned}
 \tilde{c}_0 &= \frac{\sum_{t=2}^n a_{t,0} \sum_{t=2}^n a_{t-1,0} - (n-1) \sum_{t=2}^n a_{t,0} a_{t-1,0}}{(\sum_{t=2}^n a_{t-1,0})^2 - (n-1) \sum_{t=2}^n a_{t-1,0}^2}, \\
 \tilde{c}_k &= \sqrt{2} \left(\sum_t (a_{t,k} a_{t-1,k} + b_{t,k} b_{t-1,k}) \right. \\
 & \quad \left. - \left(\sum_t a_{t,k} \sum_t a_{t-1,k} + \sum_t b_{t,k} \sum_t b_{t-1,k} \right) / (n-1) \right) \\
 & \quad / \left(\sum_t (a_{t-1,k}^2 + b_{t-1,k}^2) - \left\{ \left(\sum_t a_{t-1,k} \right)^2 + \left(\sum_t b_{t-1,k} \right)^2 \right\} / (n-1) \right), \\
 \tilde{p}_0 &= \frac{-\tilde{c}_0 \sum_{t=2}^n a_{t-1,0} + \sum_{t=2}^n a_{t,0}}{n-1}, \\
 \tilde{p}_k &= \frac{\sum_{t=2}^n a_{t,k} - \frac{1}{\sqrt{2}} \tilde{c}_k \sum_{t=2}^n a_{t-1,k}}{n-1}, \\
 \tilde{q}_k &= \frac{\sum_{t=2}^n b_{t,k} - \frac{1}{\sqrt{2}} \tilde{c}_k \sum_{t=2}^n b_{t-1,k}}{n-1}.
 \end{aligned}$$

3.3. *Forecasting electricity price curves.* The forecasts of price curves are obtained by warping back the deseasonalized curve forecasts with the respective warping functions of the same day type. For an h -day ahead forecast, we have

$$(14) \quad \hat{Y}_{t+h}^{(s)}(\tau) = \tilde{a}_{t,0} + \sum_{k=1}^{m_n} [\tilde{b}_{t,k} \phi_{2k-1}(\tau) + \tilde{a}_{t,k} \phi_{2k}(\tau)],$$

$$(15) \quad \hat{X}_{t+h}^{(s)}(\tau) = \hat{Y}_{t+h}^{(s)} \circ [\gamma^{(s)}]^{-1}(\tau),$$

where

$$\begin{aligned}
 \tilde{a}_{t,0} &= \tilde{p}_0 + \tilde{c}_0 a_{t-1,0}, \\
 \tilde{a}_{t,k} &= \tilde{p}_k + \frac{1}{\sqrt{2}} \tilde{c}_k a_{t-1,k}, \\
 \tilde{b}_{t,k} &= \tilde{q}_k + \frac{1}{\sqrt{2}} \tilde{c}_k b_{t-1,k},
 \end{aligned}$$

and $[\gamma^{(s)}]^{-1}$ is the inverse of $\gamma^{(s)}$.

4. Real data analysis.

4.1. *In-sample real time estimates.* In this section, we apply the WFAR model to perform in-sample analysis of the electricity price curves of the Nord Pool market and evaluate the performance of the WFAR model. Figure 5(a) shows the center μ_X^* (black) of the Karcher mean and the warped q_1, q_2, \dots, q_n (grey) using μ_X^* as the template in the Nord Pool market from 1 January 2013 to 31 December 2017. As can be visualized, the center μ_X^* is a good representative of the warped grey curves in terms of curve features such as broad shapes, locations and magnitudes of the peaks and valleys. Note that the underlying curves are, instead of the original price curves, SRSFs which are derivatives, that is, rates of change. Thus a

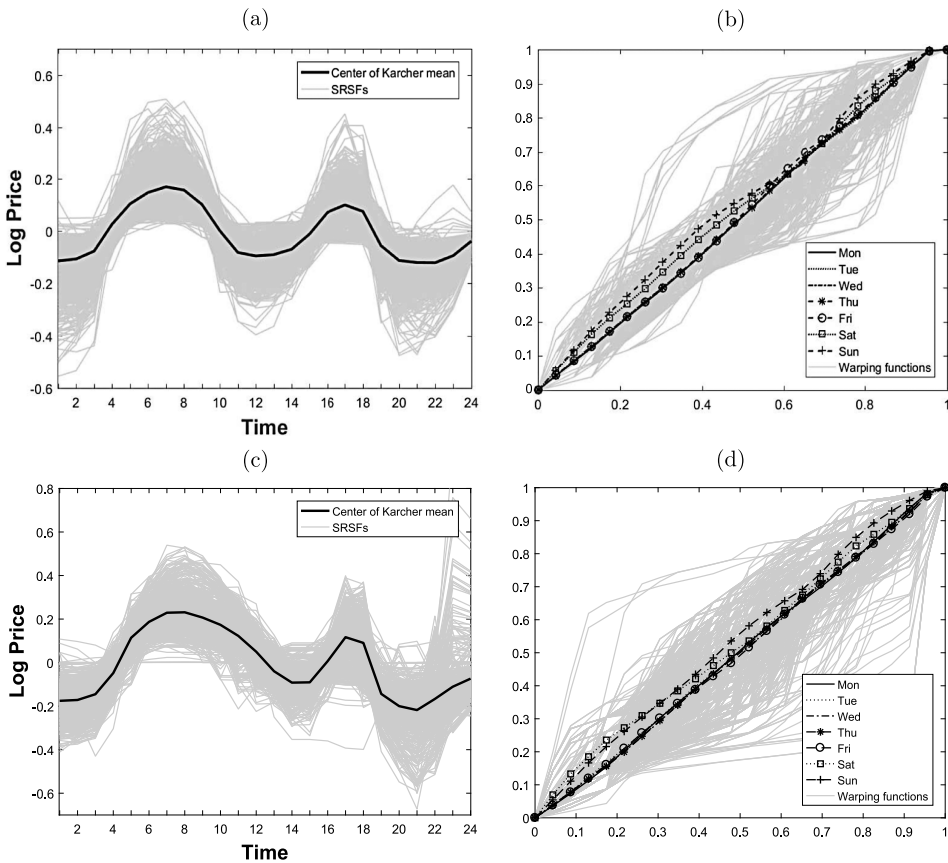


FIG. 5. SRSFs, Karcher mean and warping functions. The Nord Pool market from 1 January 2013 to 31 December 2017: (a) The center μ_X^* (black) of the Karcher mean and the warped q_1, q_2, \dots, q_n (grey) using μ_X^* as the template; (b) The Karcher means of warping functions on different days of the week. The California market from 5 July 1999 to 31 January 2001: (c) The center μ_X^* (black) of the Karcher mean and the warped q_1, q_2, \dots, q_n (grey) using μ_X^* as the template; (d) The Karcher means of warping functions on different days of the week.

high value of SRSF implies a big change in the original price while a value around zero indicates price stability. For example, it shows that the price increase speeds up starting around 14:00, slows down after 16:00 and reaches a relative stability around 18:00, which is consistent with the usual human diurnal activity. The center μ_X^* works as the template during the warping process and ensures that all the warping functions have the identity Karcher mean, that is, the diagonal line in Figure 5(b), which do not warp the curves to either left or right at all. By minimizing the \mathcal{L}^2 distance between the center μ_X^* and $(q_t \circ \gamma)\sqrt{\gamma}$ in (11), we obtain the optimal warping function γ_t for X_t , $t = 1, \dots, n$. Figure 5(b) depicts the warping functions $\gamma_1, \dots, \gamma_n$ in grey to illustrate the phase variation. As can be seen, there is noticeable daily phase variation in electricity price curves as the warping functions split much from the diagonal. The Karcher mean of the warping functions on different days of the week shows the average of the phase variation, where the Karcher mean of the warping functions on Saturday and Sunday show relatively large phase variation. As for the abnormal market, California, we observe similar behavior with slightly different diurnal pattern; see Figure 5(c) and Figure 5(d).

4.2. *Out-of-sample forecast.* In this section, we apply the proposed WFAR model to perform out-of-sample forecasts of the electricity price curves and elaborate on the usefulness of separating the seasonal phase and level amplitude variations in functional time series data. Our interest is to investigate how much the WFAR model can contribute to accuracy improvement.

4.2.1. *Forecast procedure.* We use the price data of the Nord Pool market from 28 September 2013 to 31 December 2017 and the price data of the California electricity spot market from 31 March 2000 to 31 January 2001 described in Section 2 in the forecast experiment. We employ the rolling window analysis to assess the predictive performance of the WFAR model. The rolling window size is set to be 30 days (one month). In particular, in the California market, the price data of the first 30 days from 31 March 2000 to 29 April 2000 is used for calibration when making the first forecast for 30 April 2000. In the Nord Pool market, the price data of the first 30 days from 28 September 2013 to 27 October 2013 is used for calibration when conducting the first forecast for 28 October 2013. For every day in the out-of-sample test period a day-ahead prediction has been run, forecasting the 24 hourly prices. The 1-day ahead forecast $\hat{X}_{t+1}^{(s)}$ is obtained in the warp back procedure via (15). We roll the window one day ahead each time to do the estimation and forecast until reaching the end of the sample (31 December 2017 in the Nord Pool market and 31 January 2001 in the California market).

4.2.2. *Alternative models for comparison.* Questions remain on whether accounting for seasonality in the model for electricity price forecasting is able to improve forecast accuracy. We consider AR type models with and without taking

seasonality into account. The alternative models are further categorized to univariate, multivariate and functional cases. In particular, we considered not only AR and VAR w/o seasonality, but also the ARX with the day-ahead load forecast, the minimum price of the previous day, the latest price information and three seasonal dummies as exogenous variables, in addition to several other AR type models for univariate, multivariate and functional data.

We choose the FAR model, the VAR model, the AR model, the seasonal AR (SAR) model, the ARX model. The FAR model does not take into account the seasonality in the price curves, which is however direct and effective comparison to our WFAR model for modeling the high dimensional time series in the functional domain. The VAR model serves as a representative of multivariate models for modeling the cross dependence of time series. The AR model, SAR model and ARX model are on the other hand univariate models selected for their nice forecast performance in general as elaborated in [Weron and Misiolek \(2008\)](#). Moreover, we consider two alternative AR-type models where the latest price information is utilized. In the AR* model, the lagged hourly price $X_{j,t-1}$ is replaced by $X_{24,t-1}$, that is, the last known price from the previous day. Similarly, in the ARX* model, the minimum price MinPrice_{t-1} is replaced by $X_{24,t-1}$. These two models facilitating more recent price information are expected to improve forecast accuracy, especially for the early morning hours. All the alternative models adopt the rolling window technique with the same setting as in the WFAR model.

1. Functional autoregressive (FAR) model: the functional time series model is given by

$$(16) \quad X_t(\tau) - \mu(\tau) = \rho(X_{t-1}(\tau) - \mu(\tau)) + \varepsilon_t(\tau),$$

where $X_t(\tau)$ denotes the log price curve at time t , $\mu(\tau)$ is mean function, ρ is a Hilbert–Schmidt operator that captures the serial dependence; $\varepsilon_t(\tau)$ is a strong \mathcal{H} -white noise with zero mean and finite second moment.

2. Vector autoregressive model (VAR): The multivariate time series model is given by

$$(17) \quad \mathbf{X}_t = C + A\mathbf{X}_{t-1} + \varepsilon_t,$$

where $\mathbf{X}_t \in \mathbb{R}^d$ denotes the vector of the $d = 24$ hourly price series, $C \in \mathbb{R}^{d \times 1}$ refers to the intercept and $A \in \mathbb{R}^{d \times d}$ is the VAR matrix capturing the serial cross-dependence among the multiple series.

3. Autoregressive (AR) model and its variations including AR* model, seasonal AR (SAR) model and AR model with exogenous variable (ARX and ARX*): These univariate models estimate and forecast the log prices at each hour separately and independently. Though ignoring cross-dependence in the multiple

series, they produce good forecast accuracy due to parsimony in parameters.

AR model: $X_{j,t} = \phi_{j,0} + \phi_{j,1}X_{j,t-1} + \varepsilon_{j,t},$

AR* model: $X_{j,t} = \phi_{j,0} + \phi_{j,24}X_{24,t-1} + \varepsilon_{j,t},$

SAR model: $X_{j,t} = \phi_{j,0} + \phi_{j,1}X_{j,t-1} + \phi_{j,2}X_{j,t-2} + \phi_{j,3}X_{j,t-7} + \varepsilon_{j,t},$

ARX model: $X_{j,t} = \phi_{j,0} + \phi_{j,1}X_{j,t-1} + \phi_{j,2}X_{j,t-2} + \phi_{j,3}X_{j,t-7}$
 $+ \theta_{j,1}\text{MinPrice}_{t-1} + \theta_{j,2}\text{LoadForecast}_{j,t}$
 $+ d_{j,1}\text{Mon} + d_{j,2}\text{Sat} + d_{j,3}\text{Sun} + \varepsilon_{j,t},$

ARX* model: $X_{j,t} = \phi_{j,0} + \phi_{j,1}X_{j,t-1} + \phi_{j,2}X_{j,t-2} + \phi_{j,3}X_{j,t-7}$
 $+ \theta_{j,24}X_{24,t-1} + \theta_{j,2}\text{LoadForecast}_{j,t}$
 $+ d_{j,1}\text{Mon} + d_{j,2}\text{Sat} + d_{j,3}\text{Sun} + \varepsilon_{j,t},$

where $X_{j,t} \in \mathbb{R}$ denotes the single series of log price at hour j , $j = 1, \dots, d$, MinPrice_{t-1} denotes the minimum price of the previous day and $\text{LoadForecast}_{j,t}$ denotes the load forecast of the forecasted day. The exogenous variables include MinPrice_{t-1} and $\text{LoadForecast}_{j,t}$. The dummy variables include Mon, Sat and Sun, which denote Mondays, Saturdays and Sundays, respectively.

As mentioned, FAR and WFAR, though defined in the functional domain, avoid overfitting problem by reducing in parameter space via sieve. We list the number of parameters in the models in Table 1. The WFAR model and FAR model have the smallest number of parameters, compared to 48 for the AR and AR* model, 96 for the SAR model, 216 for the ARX and 215 for ARX* model (one less than ARX as when $j = 24$, $X_{j,t-1} = X_{24,t-1}$, that is, the lagged one price is the last

TABLE 1

The parameters in WFAR model and alternative models. WFAR model and FAR model both have the smallest number of parameters of all the considered models

| Model | The parameters in each model | # Parameters for # 24 hourly price forecasts |
|-------|--|--|
| WFAR | $c_0, c_k, p_0, p_k, q_k, 1 \leq k \leq 11$ | 35 |
| FAR | $c_0, c_k, p_0, p_k, q_k, 1 \leq k \leq 11$ | 35 |
| VAR | $C_{24 \times 1}, A_{24 \times 24}$ | 600 |
| AR | $\phi_{j,0}, \phi_{j,1}, j = 1, \dots, 24.$ | 48 |
| AR* | $\phi_{j,0}, \phi_{j,24}, j = 1, \dots, 24.$ | 48 |
| SAR | $\phi_{j,0}, \phi_{j,1}, \phi_{j,2}, \phi_{j,3}, j = 1, \dots, 24.$ | 96 |
| ARX | $\phi_{j,0}, \phi_{j,1}, \phi_{j,2}, \phi_{j,3}, \theta_{j,1}, \theta_{j,2}, d_{j,1}, d_{j,2}, d_{j,3} j = 1, \dots, 24.$ | 216 |
| ARX* | $\phi_{j,0}, \phi_{j,1}, \phi_{j,2}, \phi_{j,3}, \theta_{j,24}, \theta_{j,2}, d_{j,1}, d_{j,2}, d_{j,3} j = 1, \dots, 24.$ | 215 |

known price of of the previous day) and 600 for the VAR model given 24 prices on each day.

4.2.3. *Measures of forecast comparison.* We use the root mean squared error (RMSE) as indicators of forecast performance. We calculate the RMSE of the entire forecasts and the error reduction, defined as the relative ratio of the daily average RMSE between each alternative model and the WFAR model as shown in equation (19) by WFAR model and all the alternative models.

$$(18) \quad \text{RMSE}_{,j} = \sqrt{\sum_{t=1}^N (\hat{x}_{t,j} - x_{t,j})^2 / N},$$

$$(19) \quad \text{Err Reduction} = \frac{\text{Average RMSE} - \text{Average RMSE of WFAR}}{\text{Average RMSE of WFAR}}$$

for any $j \in \{1, 2, \dots, 24\}$, where $\hat{x}_{t,j}$ is the forecast value at hour j on day t and $x_{t,j}$ is the true observed value. N is the total number of days forecasted.

To test statistical significance of forecast accuracy of the WFAR model, we use the Diebold–Mariano test, which formally investigates the relative performance of one predictive model over the alternatives (Diebold and Mariano (1995)). The DM test statistic is calculated as follows:

$$(20) \quad \text{DM}_{12} = \frac{\bar{d}_{12}}{\hat{\sigma}_{\bar{d}_{12}}},$$

where $\bar{d}_{12} = \frac{1}{24N} \sum_{t=1}^N \sum_{j=1}^{24} d_{1,2,t,j}$ is the sample mean of the loss differential, which is defined as the difference of the squared forecast errors of the two considered models, model 1 (alternative) and model 2 (WFAR)

$$(21) \quad d_{1,2,t,j} = \hat{\varepsilon}_{1,t,j}^2 - \hat{\varepsilon}_{2,t,j}^2,$$

where $\hat{\varepsilon}_{k,t,j} = \hat{x}_{k,t,j} - x_{k,t,j}$ is the forecast error of hour j on day t of model k , $k = 1, 2$. $\hat{\sigma}_{\bar{d}_{12}}$ is an unbiased estimate of the standard deviation of \bar{d}_{12} .

In addition, we conduct the multivariate (also called vectorized) Diebold–Mariano test; see Ziel and Weron (2018) and Uniejewski, Weron and Ziel (2018). The multivariate DM test statistic is calculated as follows:

$$(22) \quad \text{DM}_{12} = \frac{\bar{D}_{12}}{\hat{\sigma}_{\bar{D}_{12}}},$$

where $\bar{D}_{12} = \frac{1}{N} \sum_{t=1}^N d_{1,2,t}$ is the sample mean of the loss differential $d_{1,2,t} = \|\hat{\varepsilon}_{1,t}\|^2 - \|\hat{\varepsilon}_{2,t}\|^2$, where $\hat{\varepsilon}_{k,t}$ is the vector of the forecast errors of all the 24 hours on day t for model k and $\|\hat{\varepsilon}_{k,t}\| = \sum_{j=1}^{24} |\hat{x}_{k,t,j} - x_{k,t,j}|$. Again, $\hat{\sigma}_{\bar{D}_{12}}$ is an unbiased estimate of the standard deviation of \bar{D}_{12} .

TABLE 2

RMSE of the 1-day ahead forecasts for hourly electricity log prices using the WFAR model and the alternatives for Nord Pool market. The relative error reduction of alternative models to WFAR is from -10.7% to 266.5%

| Hour | WFAR | FAR | VAR | AR | AR* | SAR | ARX | ARX* |
|---------------|--------------|--------------|--------|--------------|--------------|-------|--------------|--------------|
| 1 | <u>0.047</u> | 0.048 | 0.110 | 0.060 | 0.030 | 0.087 | 0.088 | 0.040 |
| 2 | <u>0.059</u> | 0.061 | 0.139 | 0.070 | 0.038 | 0.087 | 0.088 | 0.045 |
| 3 | <u>0.067</u> | 0.068 | 0.178 | 0.077 | 0.046 | 0.090 | 0.094 | 0.055 |
| 4 | <u>0.073</u> | 0.073 | 0.206 | 0.083 | 0.054 | 0.098 | 0.106 | 0.070 |
| 5 | <u>0.070</u> | 0.071 | 0.197 | 0.080 | 0.054 | 0.089 | 0.097 | 0.068 |
| 6 | <u>0.064</u> | 0.066 | 0.202 | 0.074 | 0.057 | 0.080 | 0.080 | 0.067 |
| 7 | <u>0.066</u> | 0.071 | 0.231 | 0.077 | 0.066 | 0.076 | 0.069 | 0.060 |
| 8 | 0.071 | 0.081 | 0.336 | 0.086 | 0.079 | 0.082 | 0.069 | 0.060 |
| 9 | 0.075 | 0.083 | 0.378 | 0.087 | 0.083 | 0.086 | 0.074 | 0.065 |
| 10 | 0.070 | 0.072 | 0.319 | 0.077 | 0.072 | 0.077 | 0.067 | 0.060 |
| 11 | 0.065 | 0.063 | 0.254 | 0.066 | 0.062 | 0.067 | 0.059 | 0.052 |
| 12 | 0.061 | 0.059 | 0.226 | 0.060 | 0.057 | 0.062 | 0.053 | 0.048 |
| 13 | 0.060 | 0.057 | 0.205 | 0.058 | 0.055 | 0.059 | 0.052 | 0.047 |
| 14 | 0.060 | 0.058 | 0.211 | 0.059 | 0.057 | 0.060 | 0.052 | 0.047 |
| 15 | 0.059 | 0.059 | 0.224 | 0.061 | 0.059 | 0.061 | 0.055 | 0.050 |
| 16 | 0.061 | 0.060 | 0.239 | 0.062 | 0.060 | 0.065 | 0.062 | 0.058 |
| 17 | 0.064 | 0.064 | 0.265 | 0.063 | 0.064 | 0.068 | 0.064 | 0.062 |
| 18 | 0.067 | 0.068 | 0.303 | 0.067 | 0.068 | 0.074 | 0.069 | 0.067 |
| 19 | 0.060 | 0.060 | 0.275 | 0.059 | 0.060 | 0.066 | 0.061 | 0.060 |
| 20 | 0.047 | 0.047 | 0.192 | 0.043 | 0.046 | 0.047 | 0.042 | 0.041 |
| 21 | 0.040 | 0.041 | 0.143 | 0.036 | 0.040 | 0.039 | 0.033 | 0.034 |
| 22 | 0.039 | 0.041 | 0.131 | 0.033 | 0.038 | 0.036 | 0.032 | 0.032 |
| 23 | 0.039 | 0.042 | 0.128 | 0.033 | 0.038 | 0.036 | 0.032 | 0.033 |
| 24 | 0.052 | 0.052 | 0.176 | 0.052 | 0.052 | 0.063 | 0.065 | 0.063 |
| Average | <u>0.060</u> | 0.061 | 0.219 | 0.063 | 0.056 | 0.069 | 0.065 | 0.053 |
| Err Reduction | – | 1.9% | 266.5% | 6.0% | –7.1% | 15.2% | 8.7% | –10.7% |

4.2.4. *Forecast results.* Table 2 presents the hourly forecast RMSE of the day-ahead forecasts of all the considered models for the Nord Pool market on the log scale. Each row presents the RMSE of price forecasts at the particular hour using the WFAR model and the alternative models, where the best forecasts are marked in bold-face. As can be seen, the WFAR model is superior in the out-of-sample forecast experiment with small average RMSE and good accuracy for 9 of the 24 hours (underlined), without considering AR* and ARX* that depend on the last known price. Specifically, WFAR outperforms the alternative models (except for AR* and ARX*) from 1:00 to 7:00, which is the period when the valley of the daily price curve often occurs; see Figure 2(a) and Figure 3(e). This implies that the separation of the seasonal phase variation, often large at features like valleys, from amplitude level variation helps to improve the forecast accuracy. The bottom

row in Table 2 shows the relative error reduction. The WFAR model has on average smaller RMSE, 0.060, than most of the considered models except for AR* and ARX* with error reduction from 1.9% (FAR) up to 266.5% (VAR) on the log scale in the normal functioning Nord Pool market, with 6.0% daily average error reduced compared to the AR model, 15.2% to the SAR model and 8.7% to the ARX model. The AR* and ARX* models as expected perform nicely for the early morning hours, while for the late hours the relative superior performance against WFAR disappears.

Table 3 reports the RMSE of the day-ahead forecasts for hourly electricity prices for the California power market on the log scale. As can be seen, the WFAR model is the most successful in the out-of-sample forecast of the California market on the log scale with the smallest average RMSE and the best accuracy for 15 of the

TABLE 3
RMSE of the 1-day ahead forecasts for hourly electricity log prices using the WFAR model and the alternatives for California market. The relative error reduction of alternative models to WFAR is from 0.7% to 362.6%

| Hour | WFAR | FAR | VAR | AR | AR* | SAR | ARX | ARX* |
|---------------|--------------|--------------|--------|--------------|--------------|-------|--------------|-------|
| 1 | 0.088 | 0.090 | 0.675 | 0.091 | 0.088 | 0.115 | 0.141 | 0.130 |
| 2 | 0.093 | 0.095 | 0.715 | 0.096 | 0.097 | 0.120 | 0.144 | 0.137 |
| 3 | 0.095 | 0.097 | 0.805 | 0.099 | 0.103 | 0.120 | 0.134 | 0.138 |
| 4 | 0.091 | 0.091 | 0.768 | 0.090 | 0.099 | 0.104 | 0.117 | 0.121 |
| 5 | 0.097 | 0.100 | 0.714 | 0.105 | 0.105 | 0.130 | 0.141 | 0.144 |
| 6 | 0.106 | 0.110 | 0.616 | 0.116 | 0.116 | 0.133 | 0.130 | 0.139 |
| 7 | 0.121 | 0.129 | 0.615 | 0.130 | 0.139 | 0.137 | 0.140 | 0.159 |
| 8 | 0.123 | 0.130 | 0.542 | 0.134 | 0.139 | 0.139 | 0.144 | 0.158 |
| 9 | 0.123 | 0.126 | 0.459 | 0.129 | 0.134 | 0.140 | 0.152 | 0.161 |
| 10 | 0.126 | 0.128 | 0.466 | 0.135 | 0.137 | 0.144 | 0.148 | 0.147 |
| 11 | 0.140 | 0.140 | 0.521 | 0.152 | 0.157 | 0.163 | 0.155 | 0.161 |
| 12 | 0.155 | 0.152 | 0.537 | 0.162 | 0.176 | 0.174 | 0.161 | 0.175 |
| 13 | 0.160 | 0.155 | 0.572 | 0.163 | 0.189 | 0.174 | 0.158 | 0.179 |
| 14 | 0.168 | 0.165 | 0.616 | 0.169 | 0.201 | 0.178 | 0.163 | 0.191 |
| 15 | 0.167 | 0.166 | 0.710 | 0.169 | 0.204 | 0.178 | 0.160 | 0.188 |
| 16 | 0.167 | 0.166 | 0.830 | 0.168 | 0.207 | 0.175 | 0.148 | 0.164 |
| 17 | 0.162 | 0.164 | 0.613 | 0.166 | 0.204 | 0.176 | 0.149 | 0.159 |
| 18 | 0.171 | 0.172 | 0.559 | 0.176 | 0.209 | 0.203 | 0.190 | 0.192 |
| 19 | 0.164 | 0.166 | 0.526 | 0.177 | 0.198 | 0.207 | 0.196 | 0.197 |
| 20 | 0.165 | 0.165 | 0.535 | 0.174 | 0.193 | 0.200 | 0.197 | 0.204 |
| 21 | 0.157 | 0.158 | 0.528 | 0.167 | 0.178 | 0.194 | 0.194 | 0.196 |
| 22 | 0.126 | 0.125 | 0.503 | 0.141 | 0.143 | 0.167 | 0.164 | 0.172 |
| 23 | 0.101 | 0.100 | 0.565 | 0.098 | 0.097 | 0.115 | 0.120 | 0.130 |
| 24 | 0.099 | 0.099 | 0.657 | 0.102 | 0.102 | 0.116 | 0.129 | 0.125 |
| Average | 0.132 | 0.133 | 0.610 | 0.138 | 0.151 | 0.154 | 0.153 | 0.161 |
| Err Reduction | – | 0.7% | 362.6% | 4.5% | 14.1% | 16.9% | 16.0% | 22.1% |

24 hours of all the alternative models without exception. Once more, WFAR outperforms the alternative models from 1:00 to 11:00 (except for 1:00 and 4:00), the period when the valley of the daily price curve often occurs; see Figure 2(b) and Figure 3(f), indicating the usefulness of the separation of seasonality and amplitude variation in the price curves. The overall superior performance leads to the smallest average RMSE of WFAR (0.132), which is smaller than all the alternative FAR model without considering seasonality (0.133), VAR model (0.610), and univariate AR models w/o seasonality (AR: 0.138, AR*: 0.151, SAR: 0.154, ARX: 0.153 and ARX*: 0.161). At the hourly resolution, the RMSE of WFAR model has its minimum at 1:00 (low demand time) and its maximum at 18:00 (high demand time), respectively. In the best case, that is, hourly price forecast at 1:00, the minimum RMSE of WFAR (0.088) is 664.1% less than that of the VAR model (0.675), comparable to that of AR* model and 47.5% less than that of the ARX* model. In the case of price forecast at 18:00, the WFAR model still beats alternative models with its maximum RMSE (0.171) 226.8% less than that of the VAR model (0.559), and also less than those of the FAR, AR, AR*, SAR, ARX and ARX* models (0.172, 0.559, 0.176, 0.209, 0.203, 0.190 and 0.192, respectively). The WFAR model on average provides error reduction from 0.7% (FAR) up to 362.6% (VAR) on the log scale in the California market, with 4.5% daily average error reduced compared to the AR model, 14.1% to the AR* model, 16.9% to the SAR model, 16.0% to the ARX model and 22.1% to the ARX* model.

The AR* and ARX* models deliver less accurate forecasts for the California market although both are superiorly performing for Nord Pool. This is possibly because in the normal functioning market situation where the price level is relatively stable, the last known price does contain very useful information for forecasting. On the other hand, the California market is volatile with many price instabilities from day to day and thus the last price becomes less relevant. Instead seasonality seems to dominate the evolution of prices in California as we observed WFAR produces in general accurate forecasts at peaks hours and valleys.

We perform both the Diebold–Mariano test and the multivariate Diebold–Mariano test for the equality of the forecast accuracy of each alternative model with the WFAR model as benchmark. Table 4 reports the test statistics and the corresponding p -values of the Diebold–Mariano test. Except AR* and ARX* for the Nord Pool market and FAR for the California market, the WFAR model significantly outperforms the alternative models ($p < 0.05$). Table 5 displays the test statistics and the corresponding p -values of the multivariate Diebold–Mariano test. As can be seen, except AR*, ARX* and ARX model, the WFAR model significantly outperforms the alternatives ($p < 0.05$) in both the Nord Pool market and the California market. The WFAR model is robust to the selection of window size by delivering similar accuracy for various lengths of rolling window.

We also considered a parallel analysis based on inverting the log transformed forecasts, and the relative accuracy was quite similar.

TABLE 4

Diebold–Mariano test statistics and p-values for Nord Pool market and California market

| Model | Nord Pool market | | California market | |
|-------|------------------|-----------------|-------------------|-----------------|
| | DM statistics | <i>p</i> -value | DM statistics | <i>p</i> -value |
| FAR | 11.950 | 0.000 | 1.877 | 0.061 |
| VAR | 16.113 | 0.000 | 16.093 | 0.000 |
| AR | 8.883 | 0.000 | 5.011 | 0.000 |
| AR* | -5.669 | 0.000 | 11.704 | 0.000 |
| SAR | 7.533 | 0.000 | 9.687 | 0.000 |
| ARX | 5.206 | 0.000 | 6.602 | 0.000 |
| ARX* | -7.708 | 0.000 | 6.660 | 0.000 |

5. Conclusion. We propose the WFAR model to forecast electricity price curves with seasonality. Our work contributes to the energy literature by proposing a novel electricity price predictive model that simultaneously accounts for cross time-dependence and seasonal variations of the large dimensional data. Our work also contributes to the functional time series literature by separating phase variation (seasonality) and amplitude variation (time evolution). We investigate the forecast performance of the proposed WFAR model in the Nord Pool market and the California electricity market. The forecasting results allow us to conclude that WFAR model provides stable and generally good accuracy in EPF. In addition, the WFAR model is general and can be used for modeling and forecasting other functional time series with seasonality. It is worth mentioning the WFAR model is unable to deal with trends over time. For the trended data, WFAR is ready to be used after removing the trend. Furthermore, including significant exogenous variable such as load could probably enhance the forecast performance of WFAR. It

TABLE 5

Multivariate Diebold–Mariano test statistics and p-values for Nord Pool market and California market

| Model | Nord Pool market | | California market | |
|-------|------------------|-----------------|-------------------|-----------------|
| | DM statistics | <i>p</i> -value | DM statistics | <i>p</i> -value |
| FAR | 6.487 | 0.000 | 2.467 | 0.014 |
| VAR | 5.943 | 0.000 | 3.413 | 0.000 |
| AR | 3.110 | 0.002 | 3.034 | 0.003 |
| AR* | -1.744 | 0.081 | 2.623 | 0.009 |
| SAR | 2.321 | 0.020 | 2.496 | 0.013 |
| ARX | -3.131 | 0.002 | 0.492 | 0.623 |
| ARX* | -5.832 | 0.000 | 0.939 | 0.348 |

is also possible to try the Warping Functional AutoRegressive model with eXogenous variable (WFARX) as future work to extend the WFAR model.

Acknowledgments. We thank the Editor, the Associate Editor and two referees, whose comments have greatly improved the scope and presentation of the paper.

REFERENCES

- AMJADY, N., DARAEPOUR, A. and KEYNIA, F. (2010). Day-ahead electricity price forecasting by modified relief algorithm and hybrid neural network. *IET Gener. Transm. Distrib.* **4** 432–444.
- AMJADY, N. and KEYNIA, F. (2009). Day-ahead price forecasting of electricity markets by mutual information technique and cascaded neuro-evolutionary algorithm. *IEEE Trans. Power Syst.* **24** 306–318.
- ANTONIADIS, A. and SAPATINAS, T. (2003). Wavelet methods for continuous-time prediction using Hilbert-valued autoregressive processes. *J. Multivariate Anal.* **87** 133–158. [MR2007265](#)
- BELLO, A., RESESES, J., MUÑOZ, A. and DELGADILLO, A. (2016). Probabilistic forecasting of hourly electricity prices in the medium-term using spatial interpolation techniques. *Int. J. Forecast.* **32** 966–980.
- BESSE, P., CARDOT, H. and STEPHENSON, D. (2000). Autoregressive forecasting of some climatic variations. *Scand. J. Stat.* **27** 673–687.
- BHATIA, R. and HOLBROOK, J. (2006). Riemannian geometry and matrix geometric means. *Linear Algebra Appl.* **413** 594–618. [MR2198952](#)
- BOOGERT, A. and DUPONT, D. (2008). When supply meets demand: The case of hourly spot electricity prices. *IEEE Trans. Power Syst.* **23** 389–398.
- BOSQ, D. (1991). Modelization, nonparametric estimation and prediction for continuous time processes. In *Nonparametric Functional Estimation and Related Topics* (G. Roussas, ed.) 509–529. Springer, Berlin.
- BOSQ, D. (2000). *Linear Processes in Function Spaces: Theory and Applications. Lecture Notes in Statistics* **149**. Springer, New York. [MR1783138](#)
- ČENCOV, N. N. (1982). *Statistical Decision Rules and Optimal Inference. Translations of Mathematical Monographs* **53**. Amer. Math. Soc., Providence, RI. [MR0645898](#)
- CHEN, Y. and LI, B. (2017). An adaptive functional autoregressive forecast model to predict electricity price curves. *J. Bus. Econom. Statist.* **35** 371–388. [MR3663780](#)
- CONTRERAS, J., ESPINOLA, R., NOGALES, F. J. and CONEJO, A. J. (2003). ARIMA models to predict next-day electricity prices. *IEEE Trans. Power Syst.* **18** 1014–1020.
- DIDERICKSEN, D., KOKOSZKA, P. and ZHANG, X. (2012). Empirical properties of forecasts with the functional autoregressive model. *Comput. Statist.* **27** 285–298. [MR2923229](#)
- DIEBOLD, F. X. and MARIANO, R. S. (1995). Comparing predictive accuracy. *J. Bus. Econom. Statist.* **13** 253–263.
- EFRON, B. (1975). Defining the curvature of a statistical problem (with applications to second order efficiency). *Ann. Statist.* **3** 1189–1242. [MR0428531](#)
- FENG, Q., HANNIG, J. and MARRON, J. (2016). A note on automatic data transformation. *Stat* **5** 82–87.
- GAILLARD, P., GOUDE, Y. and NEDELLEC, R. (2016). Additive models and robust aggregation for GEFCom2014 probabilistic electric load and electricity price forecasting. *Int. J. Forecast.* **32** 1038–1050.
- GARCIA-MARTOS, C., RODRIGUEZ, J. and SÁNCHEZ, M. (2012). Forecasting electricity prices by extracting dynamic common factors: Application to the Iberian market. *IET Gener. Transm. Distrib.* **6** 11–20.

- GASSER, T. and KNEIP, A. (1995). Searching for structure in curve samples. *J. Amer. Statist. Assoc.* **90** 1179–1188.
- GEMAN, S. and HWANG, C.-R. (1982). Nonparametric maximum likelihood estimation by the method of sieves. *Ann. Statist.* **10** 401–414. [MR0653512](#)
- GRENANDER, U. (1981). *Abstract Inference*. Wiley, New York. [MR0599175](#)
- HERNÁEZ, E. C., GIL, J. B., LEÓN, J. D. L. F., SAN ROQUE, A., RODRIGUEZ, M., GONZÁLEZ, J., GONZÁLEZ, A. and CALMARZA, A. (2006). Competitors' response representation for market simulation in the Spanish daily market. In *Modelling Prices in Competitive Electricity Markets* 21–68. Wiley, New York.
- HOWISON, S. and COULON, M. (2009). Stochastic behaviour of the electricity bid stack: From fundamental drivers to power prices. *J. Energy Mark.* **2** 29–69.
- JANCZURA, J., TRÜCK, S., WERON, R. and WOLFF, R. C. (2013). Identifying spikes and seasonal components in electricity spot price data: A guide to robust modeling. *Energy Econ.* **38** 96–110.
- JOSKOW, P. L. (2001). California's electricity crisis. *Oxford Rev. Econ. Policy* **17** 365–388.
- JUBAN, R., OHLSSON, H., MAASOUMY, M., POIRIER, L. and KOLTER, J. Z. (2016). A multiple quantile regression approach to the wind, solar, and price tracks of GEFCom2014. *Int. J. Forecast.* **32** 1094–1102.
- KANAMURA, T. and ŌHASHI, K. (2007). A structural model for electricity prices with spikes: Measurement of spike risk and optimal policies for hydropower plant operation. *Energy Econ.* **29** 1010–1032.
- KANAMURA, T. and ŌHASHI, K. (2008). On transition probabilities of regime switching in electricity prices. *Energy Econ.* **30** 1158–1172.
- KASS, R. E. and VOS, P. W. (1997). *Geometrical Foundations of Asymptotic Inference*. *Wiley Series in Probability and Statistics: Probability and Statistics* **908**. Wiley, New York.
- KNEIP, A. and GASSER, T. (1992). Statistical tools to analyze data representing a sample of curves. *Ann. Statist.* **20** 1266–1305. [MR1186250](#)
- KOKOSZKA, P. and ZHANG, X. (2010). Improved estimation of the kernel of the functional autoregressive process. Technical report, Utah State Univ., Logan, UT.
- KOOPMAN, S. J., OOMS, M. and CARNERO, M. A. (2007). Periodic seasonal Reg-ARFIMA-GARCH models for daily electricity spot prices. *J. Amer. Statist. Assoc.* **102** 16–27. [MR2345529](#)
- LIEBL, D. (2013). Modeling and forecasting electricity spot prices: A functional data perspective. *Ann. Appl. Stat.* **7** 1562–1592. [MR3127959](#)
- LÜTKEPOHL, H. (2005). *New Introduction to Multiple Time Series Analysis*. Springer, Berlin. [MR2172368](#)
- MACIEJOWSKA, K. and NOWOTARSKI, J. (2016). A hybrid model for GEFCom2014 probabilistic electricity price forecasting. *Int. J. Forecast.* **32** 1051–1056.
- MACIEJOWSKA, K., NOWOTARSKI, J. and WERON, R. (2016). Probabilistic forecasting of electricity spot prices using factor quantile regression averaging. *Int. J. Forecast.* **32** 957–965.
- MACIEJOWSKA, K. and WERON, R. (2016). Short-and mid-term forecasting of baseload electricity prices in the UK: The impact of intra-day price relationships and market fundamentals. *IEEE Trans. Power Syst.* **31** 994–1005.
- MARRON, J. S., RAMSAY, J. O., SANGALLI, L. M. and SRIVASTAVA, A. (2014). Statistics of time warping and phase variations. *Electron. J. Stat.* **8** 1697–1702. [MR3273584](#)
- MARRON, J. S., RAMSAY, J. O., SANGALLI, L. M. and SRIVASTAVA, A. (2015). Functional data analysis of amplitude and phase variation. *Statist. Sci.* **30** 468–484. [MR3432837](#)
- MOURID, T. and BENSMAÏN, N. (2006). Sieves estimator of the operator of a functional autoregressive process. *Statist. Probab. Lett.* **76** 93–108. [MR2213247](#)
- NOGALES, F. J., CONTRERAS, J., CONEJO, A. J. and ESPÍNOLA, R. (2002). Forecasting next-day electricity prices by time series models. *IEEE Trans. Power Syst.* **17** 342–348.
- NOWOTARSKI, J. and WERON, R. (2015). Computing electricity spot price prediction intervals using quantile regression and forecast averaging. *Comput. Statist.* **30** 791–803. [MR3404360](#)

- PAPE, C., HAGEMANN, S. and WEBER, C. (2016). Are fundamentals enough? Explaining price variations in the German day-ahead and intraday power market. *Energy Econ.* **54** 376–387.
- RADHAKRISHNA RAO, C. (1945). Information and the accuracy attainable in the estimation of statistical parameters. *Bull. Calcutta Math. Soc.* **37** 81–91. [MR0015748](#)
- RAMSAY, J. O. and LI, X. (1998). Curve registration. *J. R. Stat. Soc. Ser. B. Stat. Methodol.* **60** 351–363. [MR1616045](#)
- SAKOE, H. and CHIBA, S. (1978). Dynamic programming algorithm optimization for spoken word recognition. *IEEE Trans. Acoust. Speech Signal Process.* **26** 43–49.
- SHAHIDEHPOUR, M., YAMIN, H. and LI, Z. (2002). *Market Operations in Electric Power Systems: Forecasting, Scheduling, and Risk Management*. Wiley, New York.
- SKANTZE, P. L. and ILIC, M. D. (2012). *Valuation, Hedging and Speculation in Competitive Electricity Markets: A Fundamental Approach*. Springer, Berlin.
- SRIVASTAVA, A., WU, W., KURTEK, S., KLASSEN, E. and MARRON, J. S. (2011). Registration of functional data using Fisher–Rao metric. arXiv preprint. Available at [arXiv:1103.3817](#).
- TANG, R. and MÜLLER, H.-G. (2008). Pairwise curve synchronization for functional data. *Biometrika* **95** 875–889. [MR2461217](#)
- UNIEJEWSKI, B., WERON, R. and ZIEL, F. (2018). Variance stabilizing transformations for electricity spot price forecasting. *IEEE Trans. Power Syst.* **33** 2219–2229.
- VEHVILÄINEN, I. and PYYKKÖNEN, T. (2005). Stochastic factor model for electricity spot price—the case of the Nordic market. *Energy Econ.* **27** 351–367.
- WANG, J.-L., CHIOU, J.-M. and MÜLLER, H.-G. (2016). Functional data analysis. *Annu. Rev. Stat. Appl.* **3** 257–295.
- WANG, K. and GASSER, T. (1997). Alignment of curves by dynamic time warping. *Ann. Statist.* **25** 1251–1276. [MR1447750](#)
- WERON, R. (2007). *Modeling and Forecasting Electricity Loads and Prices: A Statistical Approach*. Wiley.
- WERON, R. (2014). Electricity price forecasting: A review of the state-of-the-art with a look into the future. *Int. J. Forecast.* **30** 1030–1081.
- WERON, R. and MISIOREK, A. (2008). Forecasting spot electricity prices: A comparison of parametric and semiparametric time series models. *Int. J. Forecast.* **24** 744–763.
- ZIEL, F., STEINERT, R. and HUSMANN, S. (2015). Efficient modeling and forecasting of electricity spot prices. *Energy Econ.* **47** 98–111.
- ZIEL, F. and WERON, R. (2018). Day-ahead electricity price forecasting with high-dimensional structures: Univariate vs. multivariate models. *Energy Econ.* **70** 396–420.

Y. CHEN
DEPARTMENT OF MATHEMATICS
FACULTY OF SCIENCE
NATIONAL UNIVERSITY OF SINGAPORE
BLOCK S17, LEVEL 8, 2 SCIENCE DRIVE 2
SINGAPORE 117543
SINGAPORE
E-MAIL: matcheny@nus.edu.sg

J. S. MARRON
DEPARTMENT OF STATISTICS
AND OPERATIONS RESEARCH
UNIVERSITY OF NORTH CAROLINA
318 HANES HALL, CB# 3260
CHAPEL HILL, NORTH CAROLINA 27599-3260
USA
E-MAIL: marron@unc.edu

J. ZHANG
DEPARTMENT OF STATISTICS
AND APPLIED PROBABILITY
FACULTY OF SCIENCE
NATIONAL UNIVERSITY OF SINGAPORE
BLOCK S16, LEVEL 7, 6 SCIENCE DRIVE 2
SINGAPORE 117546
SINGAPORE
E-MAIL: jiejiezhang@u.nus.edu